A HIGH-RESOLUTION MODEL OF THE LITHOSPHERIC MAGNETIC FIELD OF MARS.

A. Morschhauser[1], V. Lesur[2], M. Grott[1], [1]*German Aerospace Center (DLR), Institute for Planetary Research, Rutherfordstrasse 2, 12489 Berlin, Germany*, [2]*Helmholtz Centre Potsdam, German Research Centre for Geosciences (GFZ), Telegrafenberg, 14473 Potsdam, Germany*.

Introduction: We present a spherical harmonic (SH) model of the Martian lithospheric magnetic field based on Mars Global Surveyor (MGS) data [1]. We use several techniques in order to obtain a reliable and well-resolved model of the Martian lithospheric field. Static external fields were treated by a joint inversion of external and internal fields, whereas temporally variable external contributions were handled by regularizing the model using an iteratively weighted least-squares algorithm (IRLS) to approach a L1-norm [2], which allows for a better representation of strong localized magnetic anomalies as compared to the conventional L2-norm. Further, a Huber-Norm [3] was used to properly treat data outliers and the data was weighted based on an analysis of the data instead of taking the a posteriori root mean square of the misfit.

Data: We use the complete MGS vector magnetometer data set, acquired from 1999 to 2006, including the low-altitude AB as well as the high-altitude MPO data [1]. In order to reduce the influence of solar-wind induced magnetic fields, only nighttime data was selected for the mapping phase orbit [4]. For the aerobraking and science phase orbit data, we decided to use all AB data below 200 km altitude, as nighttime data is scarce below this altitude. Although the contamination by external field contributions is more significant in this case, the lower altitude of the AB data provides valuable additional information on the shorter wavelengths of the field.

Model: We express the magnetic field in terms of a scalar potential field V, thus assuming that the data was collected in a source-free region. The vector magnetic field is then expressed as the gradient of a scalar potential V, which can itself be expanded in terms of spherical harmonic (SH) functions by

$$\begin{aligned} V(r,\theta,\phi) &= V_{int}(r,\theta,\phi) + V_{ext}(r,\theta,\phi) \\ &= a \sum_{l=1}^{L_{int}} \sum_{m=-l}^{l} \left(\frac{r}{a}\right)^{l} g_l^m Y_l^m(\theta,\phi) \\ &+ \sum_{l=1}^{L_{ext}} \sum_{m=-l}^{l} \left(\frac{a}{r}\right)^{l+1} h_l^m Y_l^m(\theta,\phi) \end{aligned}$$

where (r,θ,ϕ) are spherical coordinates, a is the reference radius of the model, L_{int}, L_{ext} are the maximal SH degree and order, and g_l^m, h_l^m are the Gauss coefficients for internal and external fields, respectively. Further, Y_l^m denote the Schmidt semi-normalized spherical harmonic functions, where negative orders $(m < 0)$ are associated with $\sin(m\phi)$ terms and zero or positive orders $(m \geq 0)$ are associated with $\cos(m\phi)$ terms.

The SH model was expanded up to $L_{int} = 110$, which was determined to be adequate to sufficiently resolve the intense anomalies in the AB data. External fields were modeled separately for the day- and nightside data and maximum SH degrees of $L_{ext} = 10$ and $L_{ext} = 5$ were used for the day- and nightside data, respectively.

Inversion: The quality of the inversion depends on the proper selection of data weights, which should optimally be weighted according to the probability densitiy function (PDF) of the underlying errors, such that noisy data are given less weight than good data. In our case, these errors include measurement errors such as pointing errors and the accuracy of the fluxgate magnetometer as well as contributions of non-lithospheric fields. As these errors are difficult to quantify and to model, the underlying PDF is unknown a priori, and is usually estimated a posteriori [4]. Here, we binned the data in areas of approximately equal size and calculated the respective standard deviation for each bin. The obtained standard deviations account for errors due to temporal variations in the data if the bin size is selected appropriately, and can be used as a priori data weights.

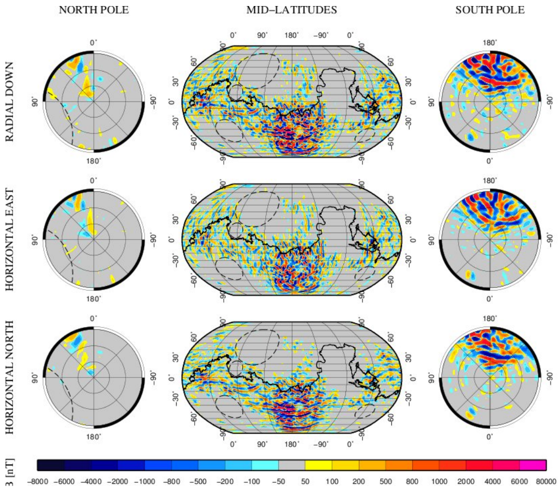

Figure 1: Map of the Martian magnetic field model evaluated at the average planetary radius of Mars (R=3393.5 km). The topographic dichotomy and major impact craters are indicated by the solid black and dashed lines, respectively.

Static non-lithospheric contributions to magnetic field data were found to be relevant at MGS orbit altitude [5] and we include a simple model of the external field. As the nature of the external field differs substantially on the day- and nightside, we used two different external field models. Further, large data outliers were treated by implementing a Huber-Norm [2], which allows to statistically treat data outliers instead of rejecting them a priori.

Remaining non-lithospheric field contributions generated below the MGS mapping altitude can leak into the lithospheric model and lead to strong field oscillations when the model is downward-continued to the surface. Hence, we minimize an additional constraint to suppress the leakage of external fields into the model. To do so, we use a measure of the

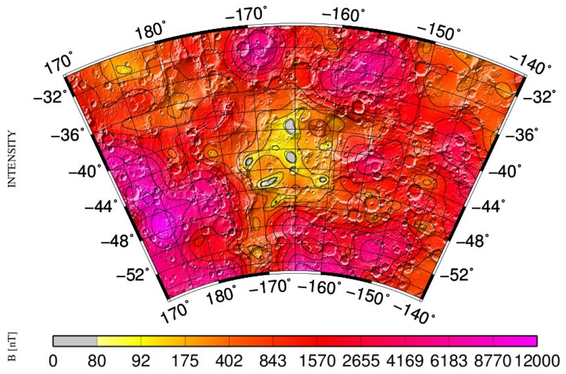

Figure 2: Map of the lithospheric field intensity at surface altitude as predicted by the presented model. The shown area is located in Terra Sirenum and shows a low-field region within an area of the strongest lithospheric fields of Mars.

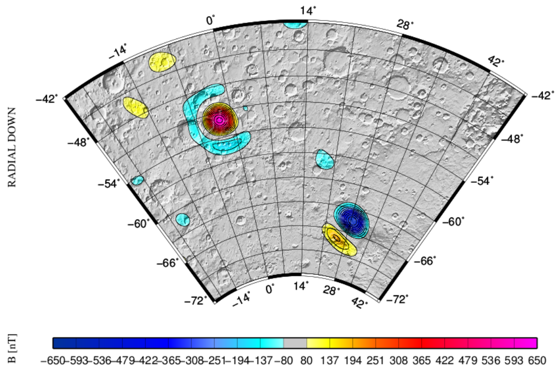

Figure 3: Radial down component of the lithospheric field at surface altitude as predicted by the presented model. The shown area is located near the south pole and shows two isolated, relatively weak anomalies. The center of the southern anomaly is located $\sim$300 km northeast of Pityusa Patera.

surface integral of the horizontal gradient of the radial magnetic field component. However, it is inevitable that some part of the lithospheric signal will also be suppressed in this way. We mitigate this effect by using an iteratively reweighted least-squares algorithm (IRLS) [2], which approaches a L1-norm, and allows for strong, localized magnetic anomalies to be better represented than with the conventional L2-norm for regularization.

Results: The lithospheric field model is shown in Fig.1 for all three vector components of the magnetic field, which has been downward-continued to surface altitude. The topographic dichotomy and the largest impact craters (Hellas, Isidis, Argyre, Utopia) are indicated by black solid and dashed lines, respectively. In agreement with previously published maps (e.g. [4,6]), it can be confirmed that the major impact craters appear to be demagnetized and the northern lowlands show generally lower magnetic fields than the southern highlands. In addition, many details are visible at high-field regions while showing a low noise level in low-field regions.

Conclusions: We presented a spherical harmonic model of the Martian lithospheric magnetic field based on the entire MPO nightside and AB/SPO data set of the Mars Global Surveyor mission. Due to its high resolution and its ability to be downward-continued to surface altitude, the presented model will help to better understand the magnetic field history of Mars. For example, the magnetic signature of smaller craters can be investigated and weaker anomalies can be resolved. In particular, a region of low-field intensity has been discovered within Terra Sirenum, surrounded by very strong fields (cf. Fig. 2). The presence of this feature could be confirmed by the electro-reflectometry (ER) map of [7], but little ER data is available in the surrounding area due to closed field lines. Although it is also visible in other published models based on the magnetometer data, it is hard to detect at higher altitudes where most of the published maps have usually been interpreted.

Another example of the ability of the new model to resolve comparatively weak features is given in Fig. 3, where two isolated anomalies near the South Pole are shown. These anomalies show no obvious correlation with geological structure, but will certainly be very useful in determining paleopoles and the magnetization of the underlying crust in the future, as their signal is not disturbed by nearby sources. Again, although these anomalies are visible in other models as well as in the ER data, they are too weak to be confidently identified at the MPO orbit altitude of 400 km. Other possible applications of the new lithospheric field model could include new estimates of the Martian lithospheric magnetization, or the investigation of the magnetic signature of impact craters down to possibly 200 km in diameter.

When interpreting the map at surface altitude, it should be kept in mind that the model resolution is limited by the maximum SH degree, corresponding to roughly 190 km at the surface, and the actual litospheric field could contain much finer structure than can be resolved with this model.

Acknowledgements: This work has been supported by the German Research Foundation (DFG) within the Priority Program SPP1408 “Planetary Magnetism”.

References [1] Acuña et al., *J. Geophys. Res.*, 106(E10), 23403-23417, 2001. [2] Farquharson and Oldenburg, *Geophys. J. Int.*, 134,213-227, 1998. [3] Huber, *Ann. Math. Stat.*, A6, 813-827, 1964. [4] Cain et al., *J. Geophys. Res.*, 108(E2), doi:10.1029/ 2000JE 001487, 2003. [5] Ferguson et al., *Geophys. Res. Lett.*, 32, L16105, doi:10.1029/ 2004GL021964, 2005. [6] Langlais et al., *J. Geophys. Res.*, 109(E02008), doi:10.1029/ 2003JE002048, 2004. [7] Lillis et al., *Icarus*, 194, 575-596. 2008.